DOI: 10.1002/ejic.200900326

One-Dimensional Coordination Polymers of Mn^{II}, Cu^{II}, and Zn^{II} Supported by Carboxylate-Appended (2-Pyridyl)alkylamine Ligands – Structure and Magnetism

Himanshu Arora,[a] Francesc Lloret,[b] and Rabindranath Mukherjee*[a]

Keywords: Coordination polymers / Crystal structures / Noncovalent interactions / Magnetic properties / Antiferromagnetic coupling / Carboxylate ligands / Bridging ligands / Structure elucidation

Four new complexes $[Mn^{II}(L^1OO)(H_2O)][ClO_4]\cdot 2H_2O$ (**1**), $[Zn^{II}(L^1OO)][ClO_4]\cdot 2H_2O$ (**2**), $[Cu^{II}(L^3OO)][CF_3SO_3]\cdot H_2O$ (**3**), and $[Zn^{II}(L^3OO)][ClO_4]$ (**4**) (L^1OO^- = 3-[(2-(pyridine-2-yl)-ethyl){2-(pyridine-2-yl)methyl}amino]propionate; L^3OO^- = 3-[(2-(pyridine-2-yl)ethyl){(dimethylamino)ethyl}amino]propionate) have been synthesized and characterized by elemental analysis, IR, and UV/Vis spectroscopy. Structural analysis revealed that **1**, **3**, and **4** are one-dimensional chain-like coordination polymers. In **1** distorted octahedral MnN_3O_3 and in **3** square-pyramidal CuN_3O_2 coordination is satisfied by three nitrogen atoms and an appended carboxylate oxygen atom of the ligand, and an oxygen atom belonging to the carboxylate group of an adjacent molecule. In **4** trigonal bipyramidal ZnN_3O_2 coordination environment is provided by two nitrogen atoms and an appended carboxylate oxygen atom of the ligand in the equatorial plane, and the two axial positions are satisfied by a tertiary amine nitrogen and an oxygen atom belonging to the carboxylate group of an adjacent molecule. In **1** the Mn^{II} center is coordinated by an additional water molecule. In these complexes each monomeric unit is sequentially connected by *syn-anti* carboxylate bridges. Temperature-dependent magnetic susceptibilities for **1** and **3** are measured, revealing antiferromagnetic interactions through *syn-anti* carboxylate bridges between the M^{II} centers. Analysis of the crystal packing diagram reveals that in **1** extensive π–π stacking involving alternate pyridine rings of adjacent 1D chain exists, which eventually lead to the formation of a 2D network structure.

Introduction

In recent years coordination polymers, consisting of metal–ligand coordination compounds in which the metal centers are interconnected by organic linkers and the metal–ligand units which generate a variety of supramolecular architectures, have attracted great interest due to their diverse structural topologies and potential applications in areas of catalysis and materials science.[1] The increasing interest in this field is justified by the intellectual challenge in controlling and manipulating the self-assembly process.[2]

Magneto-structural studies on polynuclear complexes, aimed at understanding the underlying structural factors that govern the magnetic-exchange interaction between paramagnetic centers mediated by ligand bridge(s), continue to be of interest.[3–5] Polynuclear metal carboxylates[6] are good candidates for the investigation of magnetic-exchange interaction between adjacent metal ions. It is well known that the carboxylate group can bridge metal ions to give rise to a variety of polynuclear transition metal complexes, ranging from discrete entities to three-dimensional systems.[7–9] Carboxylate group can assume many types of bridging conformations, the most important being triatomic *syn-syn*, *syn-anti*, *anti-anti* and monoatomic.[10,11] The generation of binuclear systems is favored by *syn-syn* conformation whereas *syn-anti* favors the formation of extended structures with varying nuclearity. The former mediates the antiferromagnetic exchange pathway between the metal centers, while the latter favors the ferromagnetic exchange interaction with some exceptions where antiferromagnetic coupling is favored.[8]

Very recently we have shown[12] that the carboxylate-appended anionic (2-pyridyl)alkylamine ligands afforded 1D coordination polymers of Co^{II} and Cu^{II} supported by L^1OO^- (3-[(2-(pyridine-2-yl)ethyl){2-(pyridine-2-yl)methyl}amino]propionate) and a discrete Cu^{II}_4 cluster supported by L^2OO^- (3-[*N*-methyl{2-(pyridin-2-yl)ethyl}amino]propionate), providing examples of ligand denticity-controlled self-assembly process (Scheme 1). Temperature-dependent magnetic susceptibility measurements revealed (i) spin-canted antiferromagnetism in 1D coordination polymer of Co^{II}, (ii) weak antiferromagnetic exchange interaction in

[a] Department of Chemistry, Indian Institute of Technology Kanpur,
Kanpur 208016, India
Fax: +91-512-2597437
E-mail: rnm@iitk.ac.in
[b] Departament de Química Inorgànica/Instituto de Ciencia Molecular (ICMOL), Universitat de València,
Polígono de la Coma, s/n, 46980 Paterna (València), Spain
Supporting information for this article is available on the WWW under http://dx.doi.org/10.1002/ejic.200900326.

1D coordination polymer of Cu^{II}, and (iii) ferromagnetic exchange interaction in tetracopper(II) complex. Because these ligands are not expected to saturate the coordination positions around the metal ion preferring five-/six-coordination, self-assembly reactions may occur through the deprotonated carboxylate groups, leading to carboxylate-bridged polymeric one-dimensional chains. Hoping that synthetic generality of the formation of 1D coordination polymers supported by carboxylate-appended anionic (2-pyridyl)alkylamine ligands could be established, and from the aforesaid perspective in this work we have included another (2-pyridyl)alkylamine-based ligand L^3OO^- (3-[(2-(pyridine-2-yl)ethyl){(dimethylamino)ethyl}amino]propionate) (Scheme 1) with flexible carboxylate linker. Specifically, we have synthesized and characterized new one-dimensional carboxylate-bridged complexes $[Mn^{II}(L^1OO)(H_2O)][ClO_4]\cdot 2H_2O$ (**1**), $[Zn^{II}(L^1OO)][ClO_4]\cdot 2H_2O$ (**2**), $[Cu^{II}(L^3OO)][CF_3SO_3]\cdot H_2O$ (**3**), and $[Zn^{II}(L^3OO)][ClO_4]$ (**4**), with closely similar metal–ligand bonding characteristics. Complexes **1**, **3**, and **4** are structurally characterized. We present here also the magneto-structural behavior of **1** and **3**.

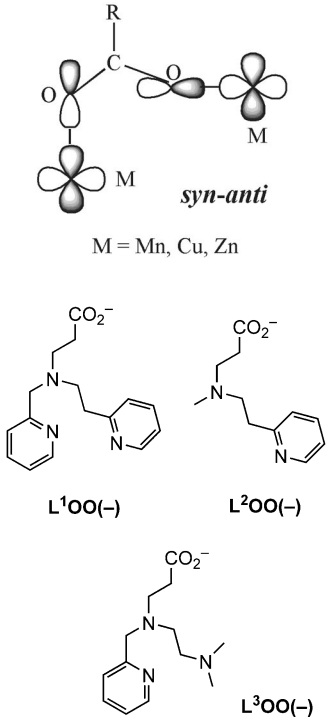

Scheme 1.

Results and Discussion

Syntheses and General Characterization

The syntheses of $[Mn^{II}(L^1OO)(H_2O)][ClO_4]\cdot 2H_2O$ (**1**), $[Zn^{II}(L^1OO)][ClO_4]\cdot 2H_2O$ (**2**), $[Cu^{II}(L^3OO)][CF_3SO_3]\cdot H_2O$ (**3**), and $[Zn^{II}(L^3OO)][ClO_4]$ (**4**) were achieved in H_2O/CH_3OH (in the case of **1** it is CH_3OH) by straightforward reaction between $[M^{II}(H_2O)_6]X_2$ [M = Mn (**1**), Zn (**2**), Zn (**4**) and X = ClO_4^-; M = Cu (**3**), X = $CF_3SO_3^-$] and lithium salt of appropriate ligand ($L^1OO^-Li^+$/$L^3OO^-Li^+$) in 1:1 metal ion–ligand stoichiometry. The syntheses of these complexes were based on the consideration that appended carboxylate group in the polydentate ligand would help in the self-assembly process and eventually would form *syn-anti* carboxylate-bridged coordination polymer (see below).

Elemental analysis, IR, and UV/Vis spectra are in excellent agreement with the above formulations of the four new complexes.

Description of Structures

Crystal Structure of $[Mn^{II}(L^1OO)(H_2O)][ClO_4]\cdot 2H_2O$ (1)

A perspective view of the cationic part of **1** is shown in Figure 1. Selected metric parameters are collected in Table 1. The ligand $L^1OO(-)$ acts as a tetradentate ligand towards a M^{II} ion and acts as a monodentate bridging ligand towards a neighboring M^{II} center, utilizing the appended carboxylate group. Each M^{II} ion is coordinated by an ethylpyridyl nitrogen N(1), a tertiary amine nitrogen N(2), a methylpyridyl nitrogen N(3), and a carboxylate oxygen O(1) from the ligand $L^1OO(-)$ and with an oxygen O(3) of H_2O. The M^{II} ions are bridged by a carboxylate group [oxygen atom O(2) belongs to the carboxylate of an adjacent molecule] to form a one-dimensional (1D) polymeric chain with an intramolecular Mn···Mn distance of 5.5663(22) Å. The angles between *trans* atoms at the metal center are in the range 158.14(15)–170.09(11)°. The *cis* angles span wide ranges 75.37(14)–101.94(12)°. Thus in **1** appreciable distortion of metal coordination environment

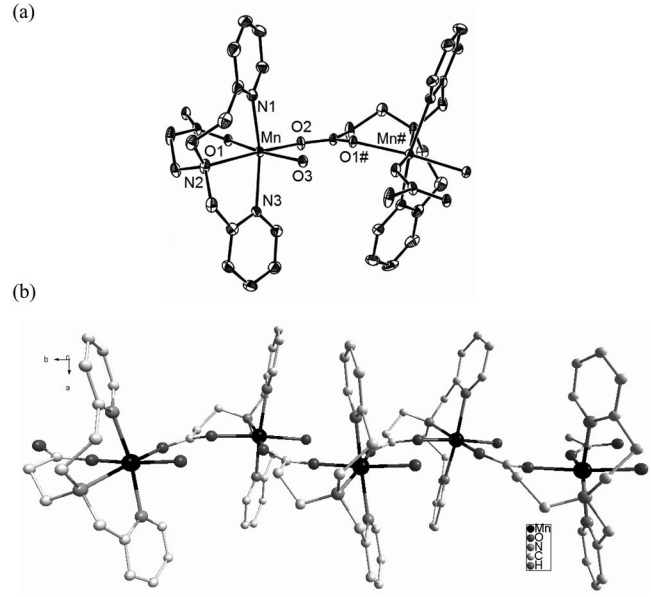

Figure 1. Perspective views of $[Mn^{II}(L^1OO)(H_2O)][ClO_4]\cdot 2H_2O$ (**1**) [only donor atoms are labeled] (a) showing metal coordination environment at two Mn^{II} centers and (b) 1D polymeric chain. All hydrogen atoms are excluded for clarity.

Table 1. Selected bond lengths [Å] and angles [°] of $[Mn^{II}(L^1OO)(H_2O)]$ $[ClO_4]\cdot 2H_2O$ (**1**), $[Cu^{II}(L^3OO)][CF_3SO_3]\cdot H_2O$ (**3**), and $[Zn^{II}(L^3OO)][ClO_4]$ (**4**).

$[Mn^{II}(L^1OO)(H_2O)]$ $[ClO_4]\cdot 2H_2O$ (**1**)			
Mn–O1	2.158(3)	Mn–O2$^{\#}$	2.126(3)
Mn–O3	2.217(3)	Mn–N1	2.227(4)
Mn–N2	2.346(4)	Mn–N3	2.230(4)
C16–O1	1.259(5)	C16–O2	1.255(5)
Mn···Mn$^{\#}$	5.5663(22)		
O1–Mn–N1	92.11(13)	O1–Mn–N2	87.94(12)
O1–Mn–N3	97.92(12)	O1–Mn–O2*	81.69(11)
O1–Mn–O3	170.14(12)	O2* –Mn–O3	88.60(12)
N1–Mn–O2*	101.15(14)	N2–Mn–O2*	167.73(13)
N3–Mn–O2*	99.47(13)	O3–Mn–N1	88.03(13)
O3–Mn–N2	101.90(13)	O3–Mn–N3	85.36(12)
N1–Mn–N2	85.69(15)	N1–Mn–N3	158.16(14)
N2–Mn–N3	75.40(14)	Mn–O1–C16	130.2(3)
Mn–O2–C16	134.5(3)	O1–C16–O2	125.3(4)
O1–C16–C15	119.0(3)	O2–C16–C15	115.7(4)
$[Cu^{II}(L^3OO)][CF_3SO_3]\cdot H_2O$ (**3**)			
Cu–O1	2.231(5)	Cu–O2	1.938(5)
Cu–N1	1.984(6)	Cu–N2	2.025(6)
Cu–N3	2.060(7)	C13–O1	1.232(8)
C13$^{\#}$–O2	1.284(8)	Cu···Cu$^{\#}$	5.281(9)
O1–Cu–N1	92.8(2)	O1–Cu–N2	92.6(2)
O1–Cu–N3	101.7(2)	O1–Cu–O2	92.26(19)
O2–Cu–N1	97.6(2)	O2–Cu–N2	175.0(2)
O2–Cu–N3	91.1(2)	N1–Cu–N2	83.3(2)
N1–Cu–N3	162.8(2)	N2–Cu–N3	86.9(2)
C13–O1–Cu	123.7(4)	Cu–O2–C13$^{\#}$	124.1(4)
O1–C13–O2*	125.1(6)	O1–C13–C12	120.3(6)
O2*–C13–C12	114.7(6)		
$[Zn^{II}(L^3OO)][ClO_4]$ (**4**)			
Zn–O1	1.998(3)	Zn–O2	2.042(3)
Zn–N1	2.073(4)	Zn–N2	2.200(3)
Zn–N3	2.100(3)	C13–O1	1.251(5)
C13–O2	1.256(5)	Zn···Zn$^{\#}$	5.4027(9)
O1–Zn–N1	136.78(14)	O1–Zn–N2	88.61(12)
O1–Zn–N3	111.78(14)	O1–Zn–O2	84.68(11)
O2–Zn–N1	104.56(13)	O2–Zn–N2	172.86(12)
O2–Zn–N3	99.92(13)	N1–Zn– N2	78.78(13)
N1–Zn–N3	108.04(14)	N2–Zn–N3	84.81(13)
Zn–O1–C13	135.4(3)	C13$^{\#}$–O2–Zn	137.8(3)
O1–C13–O2*	123.3(4)	O1–C13–C12	120.7(3)
O2* –C13–C12	116.1(3)		

$^{\#}$ Symmetry operators for the generated atoms: $-x + 3/2$, $y - 1/2$, $-z + 1/2$ for **1**; $-x + 1/2$, $y - 1/2$, $-z + 1/2$ for **2** and $-x + 1/2$, y $-1/2$, $-z + 1/2$ for **3**.
* Symmetry operators for the generated atoms: $-x + 3/2$, $y + 1/2$, $-z + 1/2$ for **1**; $-x + 1/2$, $y + 1/2$, $-z + 1/2$ for **2** and $-x + 1/2$, $y + 1/2$, $-z + 1/2$ for **3**.

from ideal geometry is apparent. Moreover, each Mn^{II} ion in **1** is displaced from the basal plane (defined by N1, O1, N3, and O3) by 0.1010(3) Å towards O(2). Notably, the Mn–O(2)–C(16)–O(1#)–Mn# bridging network appreciably deviates from planarity [dihedral angle between the planes Mn–O(2)–C(16) and Mn#–O(1#)–C(16): 22.12(1)°] and the angle between the plane of the carboxylate group coordinated to Mn# and MnN_2O_2 plane is 87.17(3)°.

The Mn–O bond lengths [2.126(3)–2.224(3) Å] are comparable to those typical of Mn–O bond lengths (2.0–2.2 Å) observed in six-coordinate Mn^{II} complexes with similar coordination environment supported by closely similar ligands.[6i,13] For the Mn–N bonds the trend is less prominent; the Mn–N(amine) bond length 2.342(4) falls within the range of reported complexes (2.25–2.35 Å) and also the average Mn–N_{py} (py = pyridine) bonds [2.228(4) Å] fall within the range of reported values (2.20–2.38 Å).[6e,13]

Crystal Structure of $[Cu^{II}(L^3OO)][CF_3SO_3]\cdot H_2O$ (3)

A perspective view of the cationic part of **3** is displayed in Figure 2 and the selected metric parameters are given in Table 1. The coordination environment of each Cu^{II} ion reveals a square-pyramidal geometry with coordination by three nitrogen atoms of L^3OO^- and an oxygen atom belonging to the carboxylate group of an adjacent molecule comprising the basal plane (N1, N2, N3, and O2) and the apical position is provided by the carboxylate oxygen atom of L^3OO^- [Cu–O(1) 2.236(3) Å]. In essence, each Cu^{II} center

is linked with adjacent Cu^{II} center by *syn-anti* carboxylate bridge to form a 1D polymeric chain with an intramolecular Cu···Cu distance of 5.281(9) Å. The CuN_3O_2 coordination sphere is slightly distorted (τ value: 0.19)[14] from an ideal geometry. In fact, each Cu^{II} ion is displaced by 0.1606(3) Å from the least-squares plane defined by the N_3O basal plane towards the carboxylate oxygen atom O(1). Moreover, the axial Cu–O(1) bond is not perfectly perpendicular to the CuN_3O plane but bent off by 4.70°. Notably, the Cu–O(2)–C(13)–O(1#)–Cu# bridging network appreciably deviates from planarity [dihedral angle between the planes Cu–O(2)–C(13) and Cu#–O(1#)–C(13): 23.40(2)°] and the angle between the plane of the carboxylate group coordinated to Cu# and CuN_3O plane is 67.27(2)°.

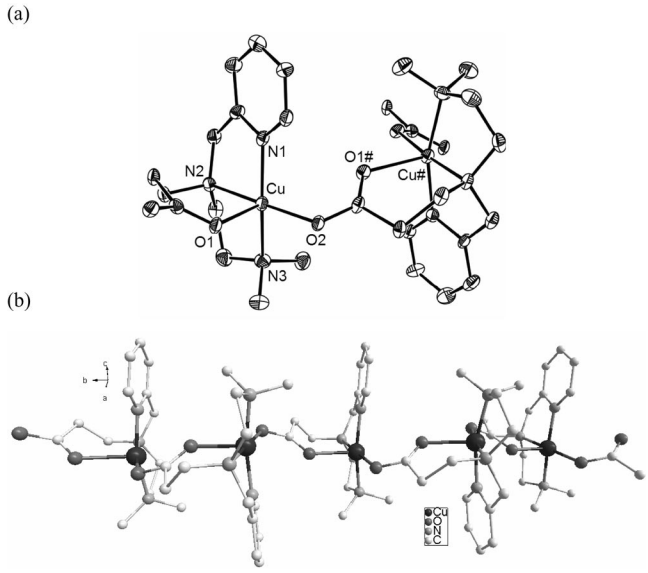

Figure 2. Perspective views of $[Cu^{II}(L^3OO)][CF_3SO_3]\cdot H_2O$ (**3**) (only donor atoms are labeled) (a) showing metal coordination environment at two Cu^{II} centers and (b) 1D polymeric chain. All hydrogen atoms are excluded for clarity.

The Cu–N_{py} bond length of 1.975(6) Å is shorter than the average Cu–N_{am} (am = tertiary amine) distance of 2.044(3) Å, providing a comparatively stronger coordination.[6j]

Crystal Structure of $[Zn^{II}(L^3OO)][ClO_4]$ (4)

A perspective view of the cationic part of **4** is shown in Figure 3 and the selected metric parameters are collected in Table 1. The coordination environment of each Zn^{II} ion reveals a trigonal-bipyramidal geometry with two nitrogen atoms and a carboxylate oxygen atom of L^3OO^- comprising the basal plane (N1, N3, and O1), whereas the apical positions are filled by an oxygen atom belonging to the carboxylate group of an adjacent molecule [Zn–O(2) 2.042(3) Å] and a tertiary amine nitrogen atom from L^3OO^- [Zn–N(2) 2.119(3) Å]. Each zinc(II) ion is coordinated by a *syn-anti* carboxylate bridge to form a 1D polymeric chain with an intramolecular Zn···Zn distance of 5.4027(9) Å. The ZnN_3O_2 coordination sphere is appreciably distorted (τ value: 0.60)[14] from ideal geometry. In fact, each Zn^{II} ion is displaced by 0.2138(1) from the least-squares plane defined by the N_2O basal plane towards the carboxylate oxygen atom O(2). The angle between the plane of the carboxylate group coordinated to Zn# and ZnN_3O plane is 78.621(12)°. Moreover, the axial Zn–O(2) bond is not perfectly perpendicular to the ZnN_2O plane but bent off by 11.47°.

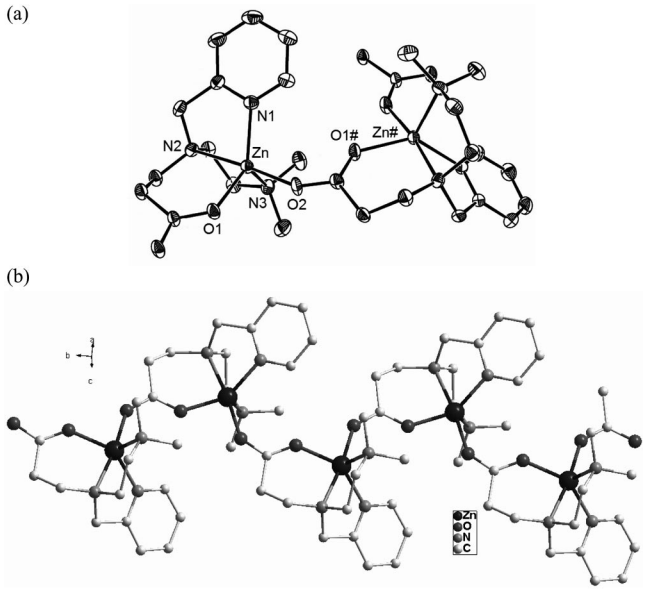

Figure 3. Perspective views of $[Zn^{II}(L^3OO)][ClO_4]$ (**4**) [only donor atoms are labeled]. (a) showing metal coordination environment at two Zn^{II} centers and (b) 1D polymeric chain. All hydrogen atoms are excluded for clarity.

The Zn–N_{py} bond length of 2.072(4) Å is shorter than the average Zn–N_{am} distance of 2.109(3) Å, providing a comparatively stronger coordination.[15] This observation is similar to that observed for **3**.

Noncovalent Interactions

A closer inspection of the crystal packing-diagram reveals that complex **1** is engaged in extensive π–π stacking interaction[16] involving alternate pyridine rings of adjacent 1D chains, leading to the formation of 2D network structure (Figure 4). The interacting pyridine rings are in a staggered conformation. The π–π stacking parameters are as follows: centroid–centroid distance: 3.6057 Å; perpendicular distance between the rings: 3.4452 Å and displacement angle (measured by the angle between the pyridine ring normal and centroid–centroid vector) β = 17.161°; dihedral angle between the planes is 0.0°.[16] The centroid–centroid distance and displacement angle in the 2D network indicate a strong parallel displaced π–π stacking between the pyridine rings.[16]

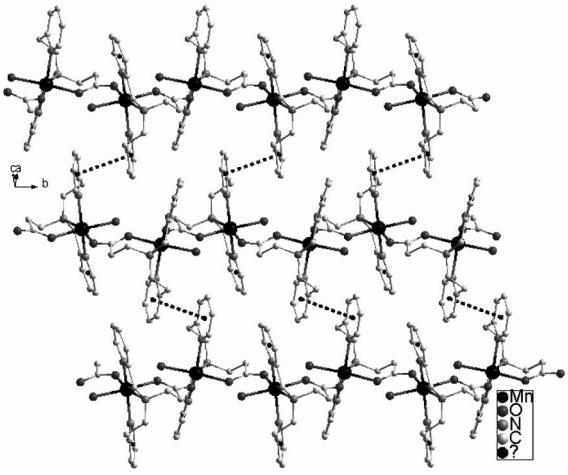

Figure 4. Formation of 2D network through π–π stacking between the one-dimensional polymeric chains of $[Mn^{II}(L^1OO)(H_2O)][ClO_4]\cdot 2H_2O$ (**1**).

Spectroscopic Properties

IR spectra of the complexes show $\nu_{as}(COO^-)$ stretching frequency in the range 1606–1611 cm^{-1} and $\nu_{sym}(COO^-)$ in the range 1419–1450 cm^{-1}. The difference between $\nu_{as}(COO^-)$ and ν_{sym} (COO^-) is about 170 cm^{-1}, suggesting a bridging coordination mode for the carboxylate group.[6e]

The absorption spectral feature of the copper(II) complex **3** in H_2O (see Figure S1 in the Supporting Information) does not support the presence of five-coordinate Cu^{II} centers in solution.[17] The asymmetric band at 14 600 cm^{-1} suggests the presence of a distorted octahedral stereochemistry around copper(II). Two possibilities exist. Either the low-energy transition falls out of the range for which the spectrum was recorded or each Cu^{II} ion, in addition to five bonding interactions, has a long Cu–O interaction due to coordination by H_2O.[12]

X-band EPR spectrum (CH_3CN/toluene; 1:1, v/v) of **1** exhibits an isotropic signal at g = 2.007 (Figure S2). The spectrum of **3** is characterized by an axial signal with $g_{\parallel}$ = 2.21 and $g_{\perp}$ = 2.08, clearly attesting the fact that the geometry around Cu^{II} in **3** is square-based and the unpaired electron resides in the $d_{x^2-y^2}$ orbital (Figure S2).[6e,17]

Magnetic Studies

Variable-temperature magnetic susceptibility measurements were performed on polycrystalline samples of **1** and **3** in the temperature range 2–300 K. Their magnetic properties under the form of $\chi_M T$ vs. T plot (χ_M being the magnetic susceptibility per metal ion) are shown in Figures 5 and 6, respectively. At room temperature, $\chi_M T$ is 4.07 $cm^3 mol^{-1} K$ (μ_{eff} = 5.68 μ_B) for **1** and 0.41 $cm^3 mol^{-1} K$ (μ_{eff} = 1.81 μ_B) for **2**. These values are close to those expected for a high-spin Mn^{II} ion (μ_{eff} = 5.91 μ_B with g = 2) and a Cu^{II} ion (μ_{eff} = 1.73 μ_B with g = 2), respectively. Upon cooling, $\chi_M T$ continuously decreases to reach a value of 1.5 $cm^3 mol^{-1} K$ (μ_{eff} = 3.46 μ_B) for **1** and 0.18 $cm^3 mol^{-1} K$ at 2 K (μ_{eff} = 1.20 μ_B) for **3**, at 2 K. This behavior is indicative of the occurrence of antiferromagnetic interactions in both compounds. The susceptibility plot does not exhibit any maximum in the temperature range studied, although an incipient maximum seems appear below 2 K in both compounds.

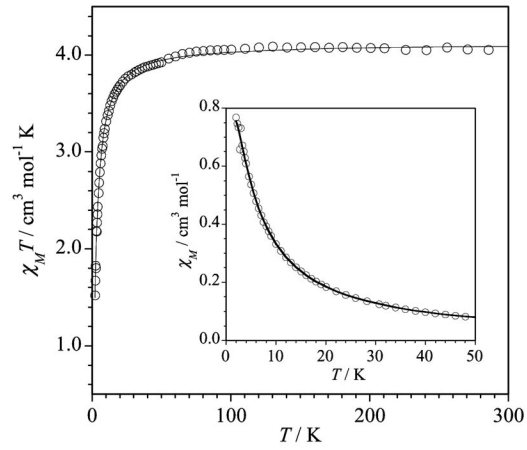

Figure 5. Plot of $\chi_M T$ vs. T for a powdered sample of $[Mn^{II}(L^1OO)(H_2O)][ClO_4]\cdot 2H_2O$ (**1**). The solid line represents the best simulation obtained with the model described in the text. The plot of χ_M vs. T is in inset.

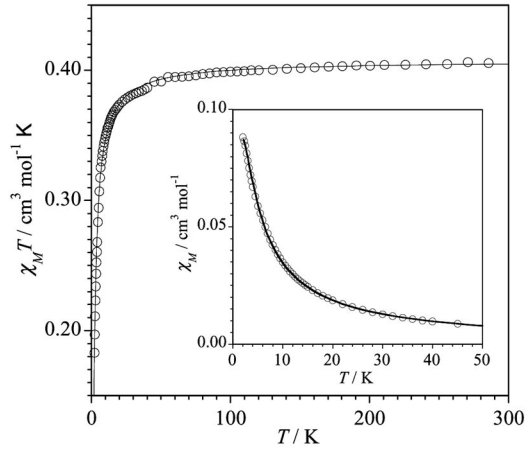

Figure 6. Plot of $\chi_M T$ vs. T for a powdered sample of $[Cu^{II}(L^3OO)][CF_3SO_3]\cdot H_2O$ (**3**). The solid lines represent the best theoretical fit, described in the text. The plot of χ_M vs. T is in inset.

Given that the structures of **1** and **3** are made up of isolated chains of metal ions, the carboxylate groups are in the *syn-anti* bridging mode, and assuming that the antiferromagnetic interactions are mainly due to intrachain exchange interactions through the carboxylato bridge, their magnetic behavior can be analyzed through the corresponding antiferromagnetic chain models. When the value of the local spin is large, it may be treated as a classical vector and an analytical expression for the magnetic susceptibility of an infinite chain of classical spins has been derived by

Fisher.[18] This expression, in which the classical spin has been scaled to a real quantum spin, S, is given in Equation (1). In practice, this expression seems fairly good for S = 5/2 and so, it can be used for Mn^{II} chains[3] such as that in **1**.

$$\chi_M = \frac{N\beta^2 g^2 S(S+1)}{3kT}\frac{1+u}{1-u} \quad (1)$$

$$\text{with } u = \coth\left[\frac{JS(S+1)}{kT}\right] - \frac{kT}{JS(S+1)}$$

The least-squares best-fit parameters for **1** are J = –0.25 cm^{-1} and g = 2.0 ($R = 2.8 \times 10^{-5}$, R is the agreement factor defined as $R = \Sigma_i[(\chi_M T)_i^{obsd} - (\chi_M T)_i^{calc}]^2/[(\chi_M T)_i^{obsd}]^2$). This J value is in agreement with values obtained for other carboxylate-bridged Mn^{II} complexes. Magneto-structural studies on polynuclear Mn^{II} complexes containing a single carboxylate bridge show the occurrence of a weak antiferromagnteic coupling[19,6h] with values of J about –0.2 cm^{-1} (*syn-anti* conformation) and –0.6 cm^{-1} (*anti-anti* conformation). For double and triple carboxylate bridges the exchange interaction is stronger[6i] ($-J \approx 0.9$ to1.7 cm^{-1} and $-J \approx 3.5$ to 4.4 cm^{-1} for doubly- and triply-bridged complexes, respectively).

In the case of a chain with S = 1/2 local spins, such as that in **3**, there is no analytical method that can be used to determine the magnetic susceptibility, in contrast to the case where a large local spin is present. This problem was solved numerically by Bonner and Fisher[20] by considering ring chains of increasing size and extrapolating to infinite. The numerical expression is given by Equation (2) and we have used it to fit the magnetic susceptibility of **3**.

$$\chi_M = \frac{N\beta^2 g^2}{kT}\frac{0.25 + 0.074975x + 0.075235x^2}{1 + 0.9931x + 0.172135x^2 + 0.757825x^3} \quad (2)$$

$$\text{with } x = \frac{|J|}{kT}$$

The least-squares best-fit parameters for **3** are J = –1.88 cm^{-1} and g = 2.08 ($R = 3.5 \times 10^{-5}$).

This weak exchange interaction is in agreement with those observed for other carboxylate-bridged Cu^{II} complexes.[21,22] It is well known that the carboxylate bridge that links the Cu^{II} ions in *syn-anti* conformation offers weak either ferro- or antiferromagnetic interactions between the metal ions.[6m,12] In addition to the conformation of the bridge, the relative orientation of the magnetic orbitals centered on the Cu^{II} ions is very unfavorable. In **3** the carboxylate bridge links an equatorial position of one Cu^{II} ion with an axial position of the adjacent Cu^{II} ion.[12] The magnetic orbital for Cu^{II} ions in a square-pyramidal surrounding is of the $d_{x^2-y^2}$-type (the x and y axes are roughly defined by the equatorial bonds). Some, admixture of the d_{z^2} orbital is present as a result of trigonal distortion. The magnetic coupling is very weak because it is the result of the interaction of a $d_{x^2-y^2}$- with a d_{z^2}-type orbitals, the latter having a very small spin density.[23] This unfavorable orientation of the magnetic orbitals centered on the Cu^{II} ions accounts for the difference between the values of J_{Mn} (–0.25 cm^{-1}) and J_{Cu} (–1.88 cm^{-1}) for **1** and **3**, respectively. The number of unpaired electrons (magnetic orbitals) on each metal center (n_{Mn} = 5 and n_{Cu} = 1) have to be taken into account in order to compare these magnetic coupling constants,[3,24] the expression being

$n_{Cu}^2 J_{Cu} = n_{Mn}^2 J_{Mn}$. In this sense, a value of J_{Cu} = 25(–0.25) = –6.25 cm^{-1} would be expected for complex **3** in the case where the equatorial–equatorial exchange pathway were involved as in the Mn^{II} complex.

Finally, these J parameters must be viewed as the upper limit values, because the possible interchain interactions have been neglected, and they could be operative through the extended π–π network (Figure 4). However, it is not possible to reproduce the experimental data for both compounds if we take into account only these interchain interactions by using a Weiss constant, $\chi_M = C/(T - \theta)$. This fact suggests that in **1** and **3** intrachain exchange interaction dominates.

Concluding Remarks

In the present study, carboxylate-appended (2-pyridyl)-alkylamine polydentate ligands L^1OO^- and L^3OO^- have been utilized to synthesize four 1D chain-like coordination polymers of Mn^{II}, Cu^{II}, and Zn^{II} utilizing *syn-anti* carboxylate bridges. While the Mn^{II} ion is six-coordinate (distorted octahedron), the Cu^{II} and Zn^{II} centers are five-coordinate (distorted square pyramidal and distorted trigonal bipyramidal, respectively). Structural analyses provide examples of the metal-ion dictated number of donor atoms around a chosen metal ion in the self-assembly process. Notably, the 1D chain of Mn^{II} coordination polymer supported by L^1OO^- forms a 2D framework, as a result of π–π stacking of pyridine rings of two adjacent layers, utilizing the coordination mode of the chosen ligands. Temperature-dependent magnetic susceptibility measurements reveal the presence of weak antiferromagnetic interactions for 1D coordination polymers of Mn^{II} and Cu^{II}. The successful syntheses of these complexes enriched the *syn-anti* carboxylate-bridged complexes not only structurally but magnetically as well. Future efforts will investigate how the stereochemical demand of this class of ligands would direct the molecular shape and control the magnetic properties of the resulting complexes. Such an endeavor is on in this laboratory.

Experimental Section

General: All reagents and solvents were obtained from commercial sources and used as received. Solvents were dried/purified following standard procedures.[25] The ligand $L^1OO^-Li^+$ was prepared as before.[12] The methodology followed to prepare $L^2OO^-Li^+$ is adapted[12] from reported procedures.[26]

Synthesis of $[Mn^{II}(L^1OO)(H_2O)][ClO_4]\cdot 2H_2O$ (1): To a magnetically stirred solution of $L^1OO^-Li^+$ (0.20 g, 0.67 mmol) in CH_3OH (10 mL) was added solid $[Mn^{II}(H_2O)_6][ClO_4]_2$ (0.24 g, 0.67 mmol) portionwise. After 3 h, the white precipitate that formed was col-

lected by filtration and dried in vacuo. Recrystallization from a mixture of H_2O/CH_3OH (v/v, 1:1) by slow evaporation afforded pale yellow crystals, suitable for structural studies; yield 0.17 g (55%). $C_{16}H_{24}ClMnN_3O_9$ (492.43): calcd. C 38.99, H 4.87, N 8.53; found C 38.76, H 4.91, N 8.61. IR (KBr; selected peaks): $\tilde{\nu}$ = 3405 [ν(OH)]; 1606 [ν_{asymm}(CO)], 1444 [ν_{symm}(CO)]; 1091 and 624 [ν(ClO_4^-)]. UV/Vis spectra [λ_{max}/nm (ε/$M^{-1}cm^{-1}$)]: 259 (8200).

Synthesis of $[Zn^{II}(L^1OO)][ClO_4]\cdot 2H_2O$ (2): To a magnetically stirred solution of $L^1OO^-Li^+$ (0.20 g, 0.67 mmol) in CH_3OH (10 mL) was added solid $[Zn^{II}(H_2O)_6][ClO_4]_2$ (0.25 g, 0.67 mmol) portionwise. After 3 h, the white precipitate that formed was collected by filtration and dried in vacuo. Recrystallization from a mixture of H_2O/CH_3OH (v/v, 1:1) by slow evaporation afforded pale yellow crystals, suitable for structural studies; yield 0.15 g (55%). $C_{16}H_{22}ClN_3O_8Zn$ (484.84): calcd. C 39.60, H 4.54, N 8.67; found C 39.26, H 4.23, N 8.97. IR (KBr; selected peaks): $\tilde{\nu}$ = 3433 [ν(OH)]; 1606 [ν_{asymm}(CO)], 1444 [ν_{symm}(CO)]; 1096 and 625 [ν(ClO_4^-)]. UV/Vis spectra [λ_{max}/nm (ε/$M^{-1}cm^{-1}$)] (H_2O): 259 (8150). ^1H NMR (400 MHz, D_2O): δ = 8.585 (d, $J_{H,H}$ = 5.6 Hz, 1 H, pyridine-H^6), 8.467 (d, $J_{H,H}$ = 5.6 Hz, 1 H, pyridine-$H^{6'}$), 7.922 (t, $J_{H,H}$ = 8 Hz, 1 H, pyridine-H^4), 7.858 (t, $J_{H,H}$ = 8 Hz, 1 H, pyridine-$H^{4'}$), 7.350–7.452 (m, 4 H, pyridine-$H^{3,3',5,5'}$), 4.376 (d, $J_{H,H}$ = 16 Hz, 1 H, -$CH_2NC_5H_4$), 3.754 (d, $J_{H,H}$ = 16 Hz, 1 H, –$CH_2NC_5H_4$), 2.843–3.266 (m, 4 H, –$CH_2CH_2NC_5H_4$), 2.095–2.658 (m, 4 H, –$CH_2CH_2CO_2$) ppm.

Synthesis of $[Cu^{II}(L^3OO)][CF_3SO_3]\cdot H_2O$ (3): To a solution of $L^3OO^-Li^+$ (0.20 g, 0.78 mmol) in H_2O (10 mL) was added solid $[Cu^{II}(H_2O)_6][CF_3SO_3]_2$ (0.36 g, 0.78 mmol) portionwise. The mixture was refluxed for 2 h and then it was kept for slow evaporation. After a few days, a crystalline product started separating out. Recrystallization was achieved from DMF/EtOAc (1:2, v/v) afforded dark blue crystals, suitable for structural studies; yield 0.20 g (60%). $C_{14}H_{22}CuF_3N_3O_6S$ (480.95): calcd. C 34.93, H 4.57, N 8.73; found C 35.21, H 4.23, N 8.27. IR (KBr; selected peaks): $\tilde{\nu}$ = 3424 [ν(OH)]; 1608 [ν_{asymm}(CO)], 1419 [ν_{symm}(CO)]; 1323 [$\nu_{asymm}(SO_3)$], 1029 [$\nu_{symm}(SO_3)$]; 1243 [$\nu_{asymm}(CF_3)$], 1170 [$\nu_{symm}(CF_3)$]. UV/Vis spectra [λ_{max}/nm (ε/$M^{-1}cm^{-1}$)] (H_2O): 685 (130), 290 (sh, 3050), 257 (6150).

Synthesis of $[Zn^{II}(L^3OO)][ClO_4]$ (4): To a stirred solution of $L^3OO^-Li^+$ (0.12 g, 0.437 mmol) in H_2O (10 mL) was added solid $[Zn^{II}(H_2O)_6][ClO_4]_2$ (0.16 g, 0.437 mmol) portionwise. After 2 h the solution was kept for slow evaporation, which afforded pale yellow crystals suitable for structural characterization; yield 0.12 g (65%). $C_{13}H_{20}ClN_3O_6Zn$ (414.8): calcd. C 37.61, H 4.82, N 10.12; found C 38.01, H 4.71, N 10.36. IR (KBr; selected peaks): $\tilde{\nu}$ = 1611 [ν_{asymm}(CO)], 1434 [ν_{symm}(CO)], 1097 and 623 [ν(ClO_4^-)]. UV/Vis spectra [λ_{max}/nm (ε/$M^{-1}cm^{-1}$)] (H_2O): 256 (6150). ^1H NMR (400 MHz, D_2O): δ = 8.401 (d, $J_{H,H}$ = 5 Hz, 1 H, pyridine-H^6), 7.922 (t, $J_{H,H}$ = 7.8 Hz, 1 H, pyridine-H^4), 7.454–7.422 (m, 2 H, pyridine-$H^{3,5}$), 4.163 (d, $J_{H,H}$ = 16.8 Hz, 1 H, –$CH_2NC_5H_4$), 3.871 (d, $J_{H,H}$ = 16.8 Hz, 1 H, –$CH_2NC_5H_4$), 2.557–3.049 (m, 4 H, –$CH_2CH_2NC_5H_4$), 2.195–2.500 (m, 4 H, –$CH_2CH_2CO_2$), 2.036 [s, 6 H, –$N(CH_3)_2$] ppm.

Caution: *Perchlorate salts of compounds containing organic ligands are potentially explosive! However, the small quantities used in our studies did not pose an hazard.*

Physical Measurements: Elemental analyses were obtained using Thermo Quest EA 1110 CHNS-O, Italy. Spectroscopic measurements were made by using the following instruments: IR (KBr, 4000–600 cm^{-1}), Bruker Vector 22. UV/Vis: Perkin–Elmer Lambda 2 and Agilent 8453 diode-array spectrophotometers. ^1H NMR spectra were obtained on JEOL JNM LA 400 (400 MHz) spectrometer using $CDCl_3$ and D_2O solution. Chemical shifts (ppm) are referenced to TMS. X-band EPR spectra were obtained on a Bruker EMX 1444 EPR spectrometer operating at 9.455 GHz (fitted with a quartz Dewar for measurements at 120 K). The spectra were calibrated with diphenylpicrylhydrazyl, DPPH (g = 2.0037).

Magnetism: The measurements on powdered samples were carried out (in València) with a MPMS-55 Quantum Design SQUID Magnetometer under an applied magnetic field of 0.01 Tesla for $T <$

Table 2. Data collection and structure refinement parameters for $[Mn^{II}(L^1OO)(H_2O)][ClO_4]\cdot 2H_2O$ (**1**), $[Cu^{II}(L^3OO)][CF_3SO_3]\cdot H_2O$ (**3**), and $[Zn^{II}(L^3OO)][ClO_4]$ (**4**).

	1	**3**	**4**
Molecular formula	$C_{16}H_{24}ClMnN_3O_9$	$C_{14}H_{22}CuF_3N_3O_6S$	$C_{13}H_{20}ClN_3O_6Zn$
M_r	492.77	480.95	415.14
Crystal color, habit	yellow, block	blue, block	yellow, block
T [K]	100(2)	293(2)	293(2)
Crystal system	monoclinic	monoclinic	monoclinic
Space group	$P2_1/n$ (#14)	$P2_1/n$ (#14)	$P2_1/n$ (#14)
a [Å]	15.333(5)	14.593(5)	13.947(3)
b [Å]	9.320(5)	9.409(5)	9.143(2)
c [Å]	15.628(5)	14.649(5)	14.050(3)
β [°]	108.525(5)	92.310(5)	112.801(4)
V [$Å^3$]	2117.6(15)	2009.8(5)	1651.5(6)
Z	4	4	4
D_c [$g\,cm^{-3}$]	1.546	1.590	1.670
μ [mm^{-1}]	0.802	1.253	1.684
F(000)	1020	988	856
Reflections collected	13440	12867	10550
Unique reflections, R_{int}	5227, 0.0403	4963, 0.0614	4050, 0.0377
Observed reflections [$I > 2\sigma(I)$]	4006	2796	2992
Goodness-of-fit on F^2	1.034	1.106	1.126
$R^{[a]}$ (R_w)$^{[b]}$ [$I > 2\sigma(I)$]	0.0699, 0.1731	0.1063, 0.2911	0.0481, 0.1115
$R^{[a]}$ (R_w)$^{[b]}$ (all data)	0.0954, 0.2011	0.1690, 0.3380	0.0738, 0.1457

[a] $R_1 = \Sigma(|F_o| - |F_c|)/\Sigma|F_o|$. [b] $wR_2 = \{\Sigma[w(|F_o|^2 - |F_c|^2)^2]/\Sigma[w(|F_o|^2)^2]\}^{1/2}$.

50 K in order to avoid saturation effects and 0.1 Tesla for $T >$ 50 K. Diamagnetic corrections were applied by using Pascal's constants.

Crystallography: For **1**, diffracted intensities was collected on a Bruker SMART APEX CCD diffractometer, with graphite-monochromated Mo-K_α (λ = 0.71073 Å) radiation at 100(2)K. Data for **3** and **4** were collected at 293 K on a Enraf Nonius MACH2 diffractometer, equipped with graphite-monochromated Mo-K_α radiation (λ = 0.71073 Å). For data reduction the Bruker Saint Plus program was used. Data were corrected for absorption and the Lorentz and polarization effects. The structures were solved with SIR-92 and refined with the SHELXL-97 package incorporated in WinGX 1.64 crystallographic collective package.[27] Anisotropic refinements were performed by full-matrix least-squares procedure on F^2. The positions of the hydrogen atoms were calculated assuming ideal geometries, but not refined. Pertinent crystallographic parameters are summarized in Table 2. For **3**, some degree of disorder was observed with triflate counteranion. Two oxygen atoms O(3) and O(4) were displaced over two positions and they were refined with site occupation factor of 0.80/0.20 and 0.75/0.25 respectively. For **3**, one peak of 3.408 e Å^{-3} was found near Cu atom at a distance of 0.941 Å and one peak of 1.66 e Å^{-3} was found near S atom at a distance of 0.860 Å. This may be due to the poor quality of the crystals chose for data collection. Intermolecular contacts of π···π stacking were examined with the DIAMOND package.[28]

CCDC-723681 (for **1**), -723682 (for **3**), and -723683 (for **4**) contain the supplementary crystallographic data for this paper. These data can be obtained free of charge from The Cambridge Crystallographic Data Centre via www.ccdc.cam.ac.uk/data_request/cif.

Supporting Information (see also the footnote on the first page of this article): UV/Vis spectra in H_2O for **3**, EPR spectra of **1** and **3**, ^{1}H NMR spectra of **2** and **4**.

Acknowledgments

We gratefully acknowledge financial support by the Department of Science & Technology, Government of India, and by the Spanish Ministerio de Educación y Ciencia (MEC) (CTQ2007-61690) and Consolider-Ingenio in Molecular Science (CSD2007–00010). R. M. is thankful to the Department of Science and Technology (DST) for a J. C. Bose Fellowship. H. A. thanks the Council of Scientific and Industrial Research, Government of India for a Senior Research Fellowship.

[1] a) M. Eddaoudi, D. B. Moler, H. Li, B. Chen, T. M. Reineke, M. O'Keeffe, O. M. Yaghi, *Acc. Chem. Res.* **2001**, *34*, 319–330; b) B. Moulton, M. R. Zaworotko, *Chem. Rev.* **2001**, *101*, 1629–1658; c) O. R. Evans, W. Lin, *Acc. Chem. Res.* **2002**, *35*, 511–522; d) S. L. James, *Chem. Soc. Rev.* **2003**, *32*, 276–288; e) C. Janiak, *Dalton Trans.* **2003**, 2781–2804; f) S. Kitagawa, R. Kitaura, S.-i. Noro, *Angew. Chem. Int. Ed.* **2004**, *43*, 2334–2375; g) N. C. Gianneschi, M. S. Masar III, C. A. Mirkin, *Acc. Chem. Res.* **2005**, *38*, 825–837; h) N. R. Champness, *Dalton Trans.* **2006**, 877–880; i) S. Natarajan, S. Mandal, *Angew. Chem. Int. Ed.* **2008**, *47*, 4798–4828.

[2] a) K. S. Murray, *Adv. Inorg. Chem.* **1995**, *43*, 261–358; b) R. E. P. Winpenny, *Adv. Inorg. Chem.* **2001**, *52*, 1–111.

[3] O. Kahn, *Adv. Inorg. Chem.* **1995**, *43*, 179–259.

[4] O. Kahn, *Molecular Magnetism*, VCH Publishers, New York, **1993**.

[5] O. Kahn, *Struct. Bonding (Berlin)* **1987**, *68*, 89–167.

[6] a) R. L. Karlin, K. Kopinga, O. Kahn, M. Verdaguer, *Inorg. Chem.* **1986**, *25*, 1786–1789; b) E. Colacio, J. P. Costes, R. Kivekäs, J. P. Laurent, J. Ruiz, *Inorg. Chem.* **1990**, *29*, 4240–4246; c) E. Colacio, J. M. Domínguez-Vera, M. Ghazi, R. Kivekäs, M. Klinga, J. M. Moreno, *Eur. J. Inorg. Chem.* **1999**, 441–445; d) C. Policar, M. Lambert, M. Cesario, I. Morgenstern-Badarau, *Eur. J. Inorg. Chem.* **1999**, 2201–2207; e) E. Colacio, M. Ghazi, R. Kivekäs, J. M. Moreno, *Inorg. Chem.* **2000**, *39*, 2882–2890; f) C. Ruiz-Pérez, Y. Rodríguez-Martín, M. Hernández-Molina, F. S. Delgado, J. Pasán, J. Sanchiz, F. Lloret, M. Julve, *Polyhedron* **2003**, *22*, 2111–2123; g) J. Pasán, F. S. Delgado, Y. Rodríguez-Martín, M. Hernández-Molina, C. Ruiz-Pérez, J. Sanchiz, F. Lloret, M. Julve, *Polyhedron* **2003**, *22*, 2143–2153; h) C. Ma, C. Chen, Q. Liu, F. Chen, D. Liao, L. Li, L. Sun, *Eur. J. Inorg. Chem.* **2003**, 2872–2879; i) S. Durot, C. Policar, G. Pelosi, F. Bisceglie, T. Mallah, J.-P. Mahy, *Inorg. Chem.* **2003**, *42*, 8072–8080 and references cited therein; j) K.-Y. Choi, Y.-M. Jeon, H. Ryu, J.-J. Oh, H.-H. Lim, M.-W. Kim, *Polyhedron* **2004**, *23*, 903–911; k) S.-i. Noro, H. Miyasaka, S. Kitagawa, T. Wada, T. Okubo, M. Yamashita, T. Mitani, *Inorg. Chem.* **2005**, *44*, 133–146; l) K.-Y. Choi, S.-Y. Park, Y.-M. Jeon, H. Ryu, *Struct. Chem.* **2005**, *16*, 649–656; m) J. Pasán, J. Sanchiz, C. Ruiz-Pérez, F. Lloret, M. Julve, *Inorg. Chem.* **2005**, *44*, 7794–7801; n) M. R. Montney, R. L. LaDuca, *Inorg. Chem. Commun.* **2007**, *10*, 1518–1522; o) Y. Zhang, H.-C. Liang, L. N. Zakharov, S. K. Das, M. M. Hetu, A. L. Rheingold, *Inorg. Chim. Acta* **2007**, *360*, 1691–1701.

[7] R. J. Doedens, *Prog. Inorg. Chem.* **1976**, *21*, 209–231.

[8] S. J. Rettig, R. C. Thompson, J. Trotter, S. Xia, *Inorg. Chem.* **1999**, *38*, 1360–1363, and references cited therein.

[9] V. Tangoluis, G. Psomas, C. Dendrinou-Samara, C. P. Raptopoulou, A. Terzis, D. P. Kessissoglou, *Inorg. Chem.* **1996**, *35*, 7655–7660.

[10] a) G. B. Deacon, R. J. Phillips, *Coord. Chem. Rev.* **1980**, *33*, 227–250; b) M. Melnik, *Coord. Chem. Rev.* **1981**, *36*, 1–44; c) M. Kato, Y. Muto, *Coord. Chem. Rev.* **1988**, *92*, 45–83.

[11] C. Oldham, in *Comprehensive Coordination Chemistry* (Eds.: G. Wilkinson, R. D. Gillard, J. A. McCleverty), Pergamon Press, Oxford, U. K., **1987**; vol. 2, pp. 435–442.

[12] H. Arora, F. Lloret, R. Mukherjee, *Inorg. Chem.* **2009**, *48*, 1158–1167, and references cited therein.

[13] H. Iikura, T. Nagata, *Inorg. Chem.* **1998**, *37*, 4702–4711.

[14] A. W. Addison, T. N. Rao, J. Reedijk, J. van Rijn, G. C. Verschoor, *J. Chem. Soc., Dalton Trans.* **1984**, 1349–1356.

[15] a) A. Majumdar, S. Shit, C. R. Choudhury, S. R. Batten, G. Pilet, D. Luneau, N. Daro, J. P. Sutter, N. Chattopadhyay, S. Mitra, *Inorg. Chim. Acta* **2005**, *358*, 3855–3864; b) W. Zhao, J. Fan, T. Okamura, W. Y. Sun, N. J. Ueyama, *J. Solid State Chem.* **2004**, *177*, 2358–2365.

[16] a) C. Janiak, *J. Chem. Soc., Dalton Trans.* **2000**, 3885–3896; b) D. L. Reger, J. R. Gardinier, R. F. Semeniuc, M. D. Smith, *Dalton Trans.* **2003**, 1712–1718; c) D. L. Reger, R. F. Semeniuc, M. D. Smith, *Cryst. Growth Des.* **2005**, *5*, 1181–1190.

[17] B. J. Hathaway, in *Comprehensive Coordination Chemistry* (Eds.: G. Wilkinson, R. D. Gillard, J. A. McCleverty), Pergamon, Oxford, **1987**, vol. *5*, pp. 533–774.

[18] M. E. Fisher, *Am. J. Phys.* **1964**, *32*, 343–346.

[19] Y. Rodríguez-Martín, M. Hernández-Molina, J. Sanchiz, C. Ruiz-Pérez, F. Lloret, M. Julve, *Dalton Trans.* **2003**, 2359–2365.

[20] J. C. Bonner, M. E. Fisher, *Phys. Rev.* **1964**, *135*, A640–A658.

[21] J. Pasán, J. Sanchiz, C. Ruiz-Pérez, F. Lloret, M. Julve, *Eur. J. Inorg. Chem.* **2004**, 4081–4090.

[22] A. Rodríguez-Fortea, P. Alemany, S. Alvarez, E. Ruiz, *Chem. Eur. J.* **2001**, *7*, 627–637.

[23] G. De Munno, M. Julve, F. Lloret, J. Cano, A. Caneschi, *Inorg. Chem.* **1995**, *34*, 2048–2053.

[24] R. Ruiz, F. Lloret, M. Julve, M. C. Muñoz, C. Bois, *Inorg. Chim. Acta* **1994**, *219*, 179–186.

[25] a) A. K. Singh, V. Balamurugan, R. Mukherjee, *Inorg. Chem.* **2004**, *43*, 6497–6502; b) A. K. Singh, R. Mukherjee, *Inorg.*

Chem. **2005**, *44*, 5813–5819; c) A. K. Sharma, F. Lloret, R. Mukherjee, *Inorg. Chem.* **2007**, *46*, 5128–5130; d) A. K. Singh, R. Mukherjee, *Dalton Trans.* **2008**, 260–270.

[26] a) S. Bhattacharya, K. Snehalatha, V. P. Kumar, *J. Org. Chem.* **2003**, *68*, 2741–2747; b) N. M. F. Carvalho, A. Horn Jr., R. B. Faria, A. J. Bortoluzzi, V. Drago, O. A. C. Antunes, *Inorg. Chim. Acta* **2006**, *359*, 4250–4258.

[27] L. J. Farrugia, WinGX version 1.64, *An Integrated System of Windows Programs For the Solution, Refinement and Analysis of Single-Crystal X-ray Diffraction Data*, Department of Chemistry, University of Glasgow, **2003**.

[28] *DIAMOND ver 2.1c*, Crystal Impact GbR, Bonn, Germany, **1999**.

Received: April 9, 2009
Published Online: June 25, 2009

